Supporting Information

Iridium(III) complexes conjugated with naproxen exhibiting potent anti-tumor activities by inducing mitochondrial damage, modulating inflammation, and enhancing immunity

Kai Xie [1], Xing-Yun Lu [1], Hou Zhu, Lin-Yuan Zhu, Rong-Tao Li* and Rui-Rong Ye*

Faculty of Life Science and Technology, Kunming University of Science and Technology, Kunming 650500, P. R. China

* Corresponding author.

E-mail addresses: rongtaolikm@163.com (R.-T. Li), yerr@mail2.sysu.du.cn (R.-R. Ye).

[1] These authors contributed equally to this work.

Supporting Experimental Methods

Cell lines and culture conditions

HeLa, HepG2, A549, A549R and LO2 were purchased from Nanjing KGI Biotech. RPMI 1640 medium was used to incubate A549, DMEM medium was used to culture LO2, HepG2, and HeLa, and cisplatin-containing DMEM medium was used to culture A549R. All five types of cells were cultured in a cell culture incubator at 37 ℃ and 5% CO_2.

MTT assay for cytotoxicity

The cells were inoculated in 96-well plates. After 24 h, the cells were co-incubated with different concentrations of **Ir-NPX-1–3**. Next, cells were placed in a cell culture incubator and continued to incubate for 44 h. 20 μL MTT was added to each well, and after 4 h, the absorbance at 590 nm was detected. Finally, the IC_{50} of the complexes was calculated using SPSS software.

Cell co-localization experiments

Ir-NPX-1–3 (20 μM) was added and incubated for 3 h. Next, the cells were co-incubated with the commercial lysosomal probe LTDR (50 nM) or the mitochondrial probe MTDR (150 nM) for 30 min. Subsequently, the cells were washed twice with PBS, and the cells were observed using a laser confocal microscope. (λ_{ex} = 405 nm for **Ir-NPX-1–3**, 633 nm for MTDR and LTDR; λ_{em} = 600 ± 20 nm for **Ir-NPX-1–3**, 665 ± 20 nm for MTDR and LTDR).

MMP analysis

The indicated concentrations of **Ir-NPX-1–3** were added to A549R cells and incubated for 6 h, then 1 mL of JC-1 (5 μg/mL) was added and co-incubated with the cells for 30 min. Cells were washed twice with PBS, and examined using laser confocal microscopy or flow cytometry. (λ_{ex} = 488 nm; λ_{em} = 530 ± 20 nm (Green), 585 ± 20 nm (Red)).

Measurement of ROS levels

Cells were incubated with different concentrations of **Ir-NPX-1–3** for 6 h. Subsequently, H_2DCFDA (10 μM) was added for a total of 15 min, and at the end of the incubation, the cells were washed twice by PBS and observed using laser confocal microscopy. (λ_{ex} = 488 nm; λ_{em} = 530 ± 20 nm).

Annexin V staining

Cells were inoculated into 6-well plates. After 24 h, cells were treated with different concentrations of **Ir-NPX-1–3** for 24 h. Then, cells were collected, centrifuged, and resuspended in PBS. Cell staining was performed according to the Annexin V-FITC Apoptosis Detection Kit. Quantification was performed by flow cytometry. (λ_{ex} = 488 nm; λ_{em} = 530 ± 20 nm).

Scratch healing assay

Cells were treated with **Ir-NPX-1–3** (1.0 μM) for 0 h, 24 h, and 48 h. A crosshatch was made inside the cell wells, the medium was aspirated and the cell debris was washed, and the scratches were subsequently observed under a fluorescence inverted microscope, and the positions of the scratches were photographed and recorded. The healing of cell scratches was recorded by fluorescence inverted microscope after 24 h and 48 h of incubation.

Colony formation experiments

Cells were cultured in 6-well plates until apposition, medium containing **Ir-NPX-1–3** was added, and incubated for 24 h. Subsequently, the culture medium was replaced with fresh medium and cultured for one week. Finally, the cells were rinsed twice with PBS and then fixed with 4% paraformaldehyde for 10 min, and the cell colony formation was observed by staining using crystal violet.

Immunogenic cell death

After treatment with the indicated concentration of **Ir-NPX-1–3** for 24 h, cells were fixed for 20 min with 4% paraformaldehyde. Then cells were washed three times with PBS and incubated with TrionX-100 for 15 min at room temperature. Subsequently, the samples were closed for 1 h with immunostaining blocking solution, washed again with PBS, the primary antibody (CRT and HMGB1) was added and placed overnight at 4 °C. After completion, the samples were incubated with the fluorescent labeled secondary antibody (Alexa Fluor 488-labeled Goat Anti-Rabbit IgG(H+L)) for 1 h at room temperature, and observed under a laser confocal microscopy. (λ_{ex} = 488 nm; λ_{em} = 530 ± 20 nm).

Determination of ATP content

Cells were treated with the indicated concentration of **Ir-NPX-1–3** for 24 h. Then the culture medium was aspirated and 200 μL of lysate was added to each well. After lysis, the samples were

centrifuged at 12000 g for 5 minutes at 4 °C to removed the supernatant. The ATP content was measured using the ATP Assay Kit According to the manufacturer's protocol.

Statistical analysis

Biological experiments were repeated more than 3 times and the mean ± SD shows the results.

Supplementary Scheme, Figures and Tables

Scheme S1 Synthetic route of **Ir-NPX-1–3**

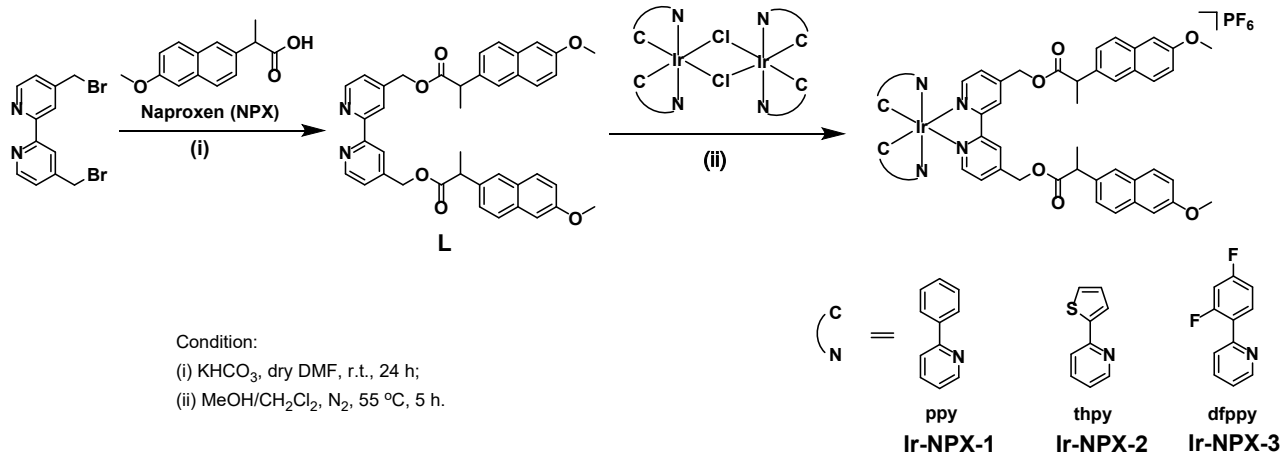

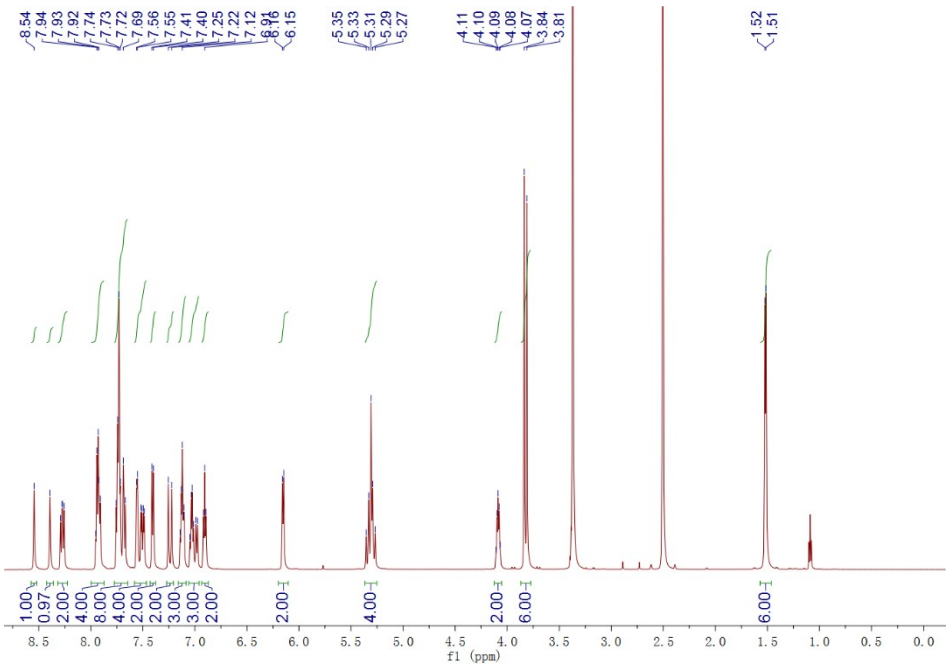

Fig. S1 ^{1}H NMR spectrum characterization of **Ir-NPX-1** in DMSO-d_6 (600 MHz, 25 ℃).

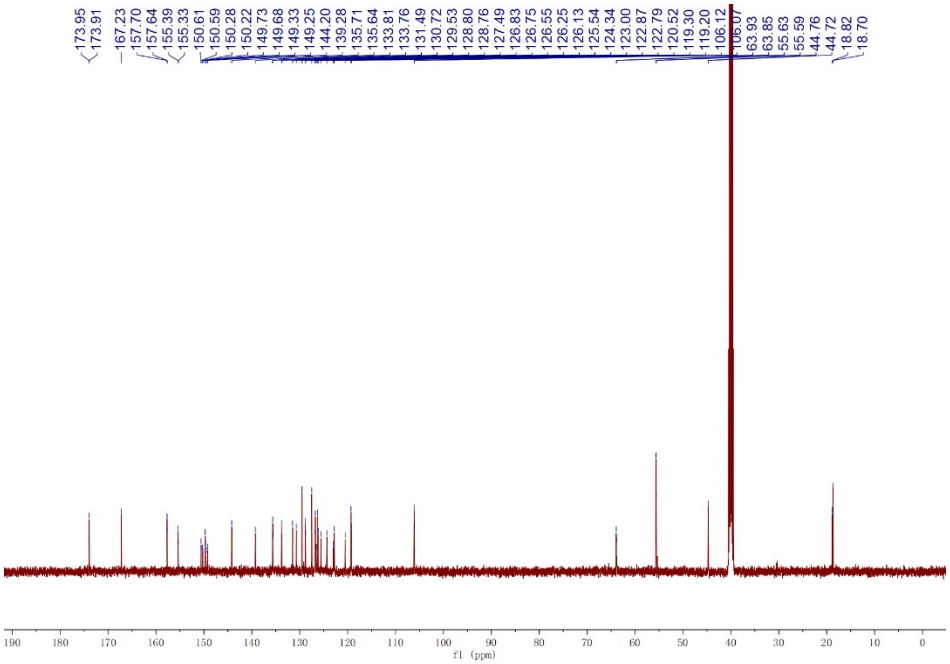

Fig. S2 ^{13}C NMR spectrum characterization of **Ir-NPX-1** in DMSO-d_6 (125 MHz, 25 ℃).

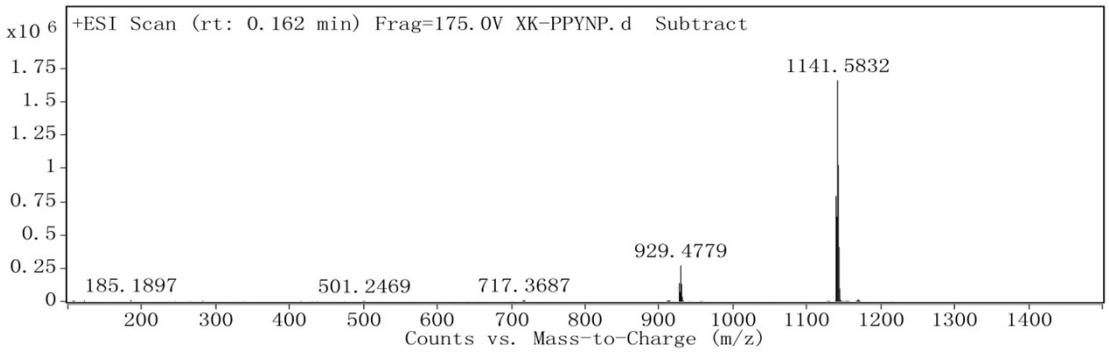

Fig. S3 ESI-HRMS characterization of **Ir-NPX-1** in CH_3OH, 1141.5832 $[M\text{-}PF_6]^+$.

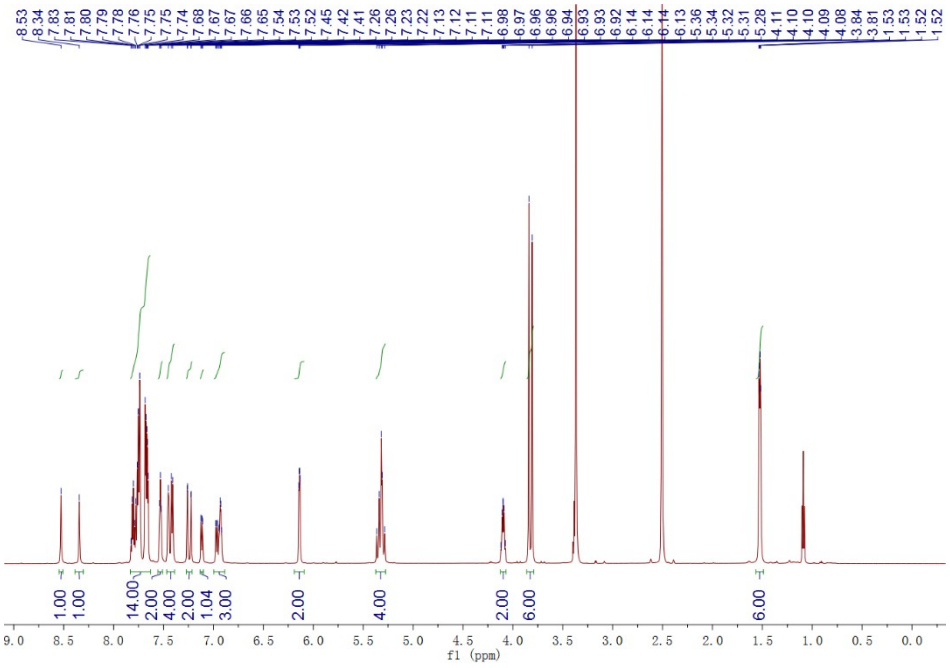

Fig. S4 ^1H NMR spectrum characterization of **Ir-NPX-2** in DMSO-d_6 (600 MHz, 25 ℃).

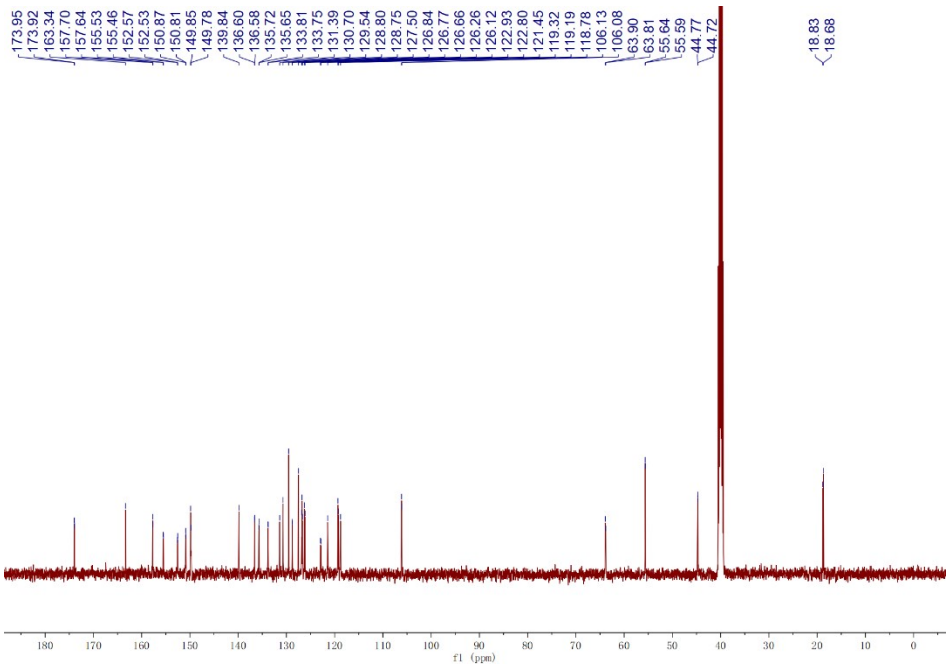

Fig. S5 ^{13}C NMR spectrum characterization of **Ir-NPX-2** in DMSO-d_6 (125 MHz, 25 ℃).

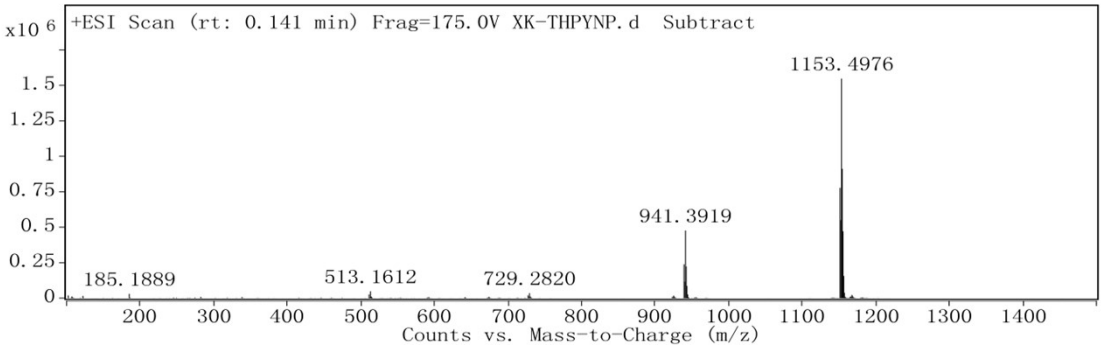

Fig. S6 ESI-HRMS characterization of **Ir-NPX-2** in CH_3OH, 1153.4976 $[M\text{-}PF_6]^+$.

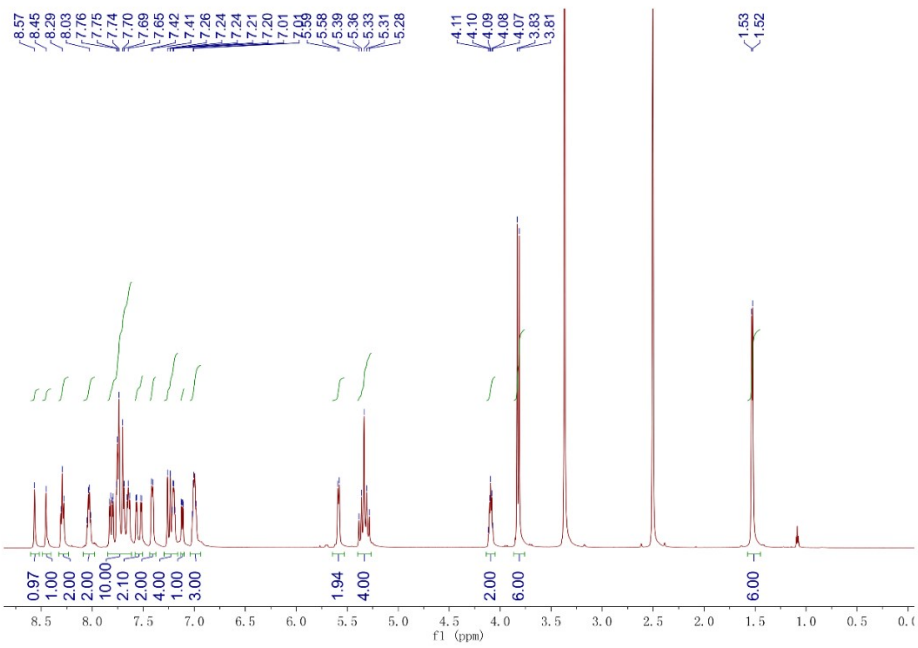

Fig. S7 ^{1}H NMR spectrum characterization of **Ir-NPX-3** in DMSO-d_6 (600 MHz, 25 ℃).

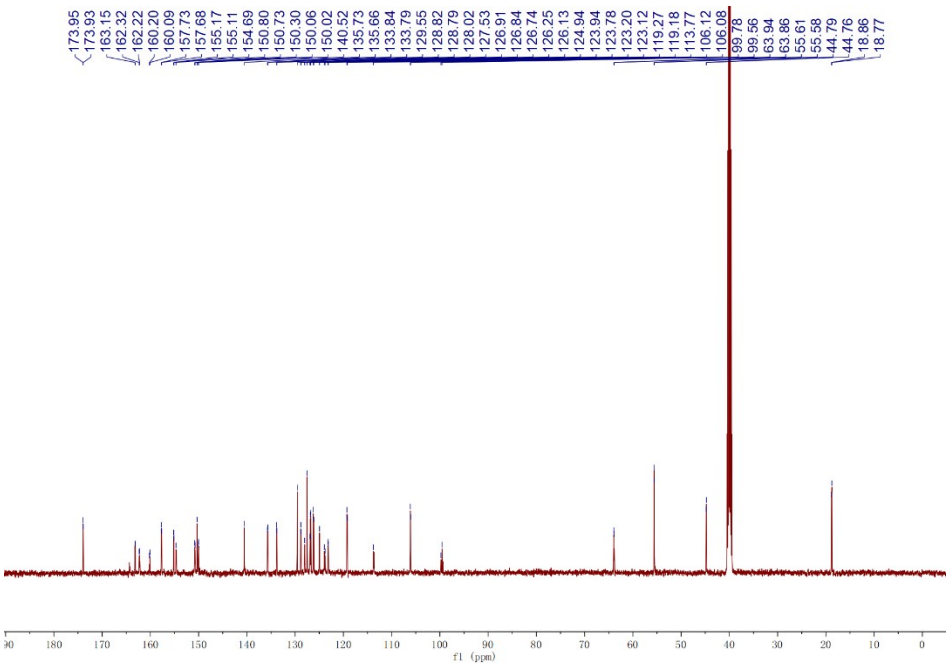

Fig. S8 ^{13}C NMR spectrum characterization of **Ir-NPX-3** in DMSO-d_6 (125 MHz, 25 ℃).

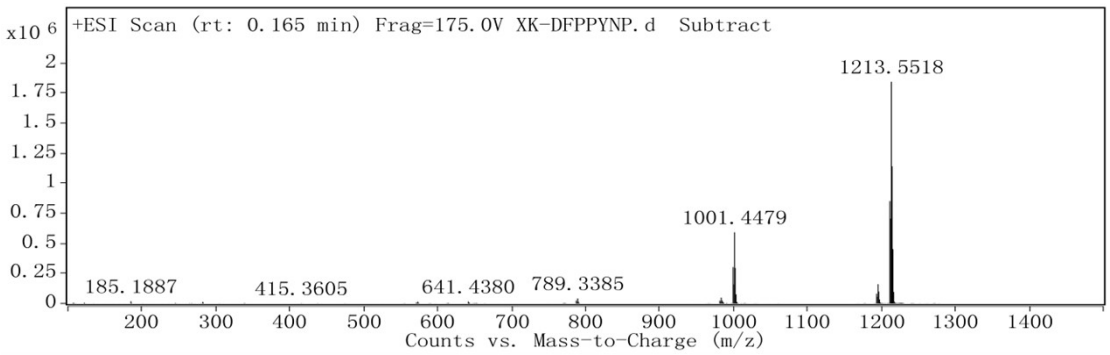

Fig. S9 ESI-HRMS characterization of **Ir-NPX-3** in CH_3OH, 1213.5518 $[M\text{-}PF_6]^+$.

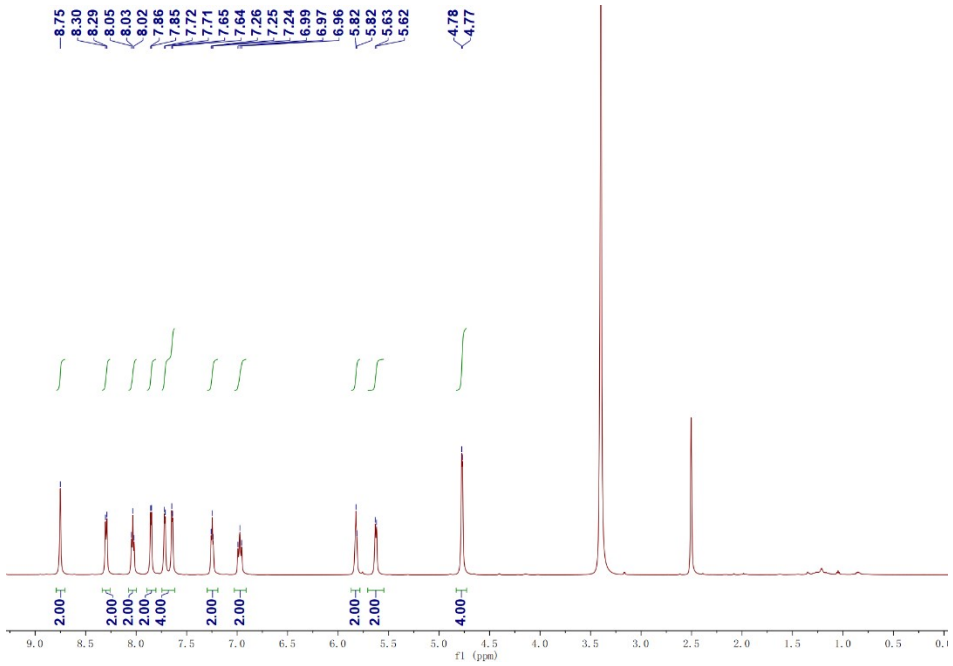

Fig. S10 ^1H NMR spectrum characterization of **Ir3** in DMSO-d_6 (600 MHz, 25 ℃).

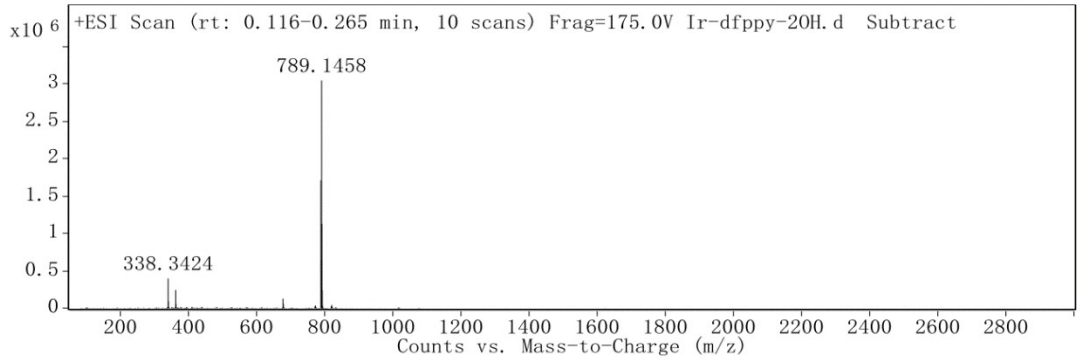

Fig. S11 ESI-HRMS characterization of **Ir3** in CH_3OH, 789.1458 $[M\text{-}PF_6]^+$.

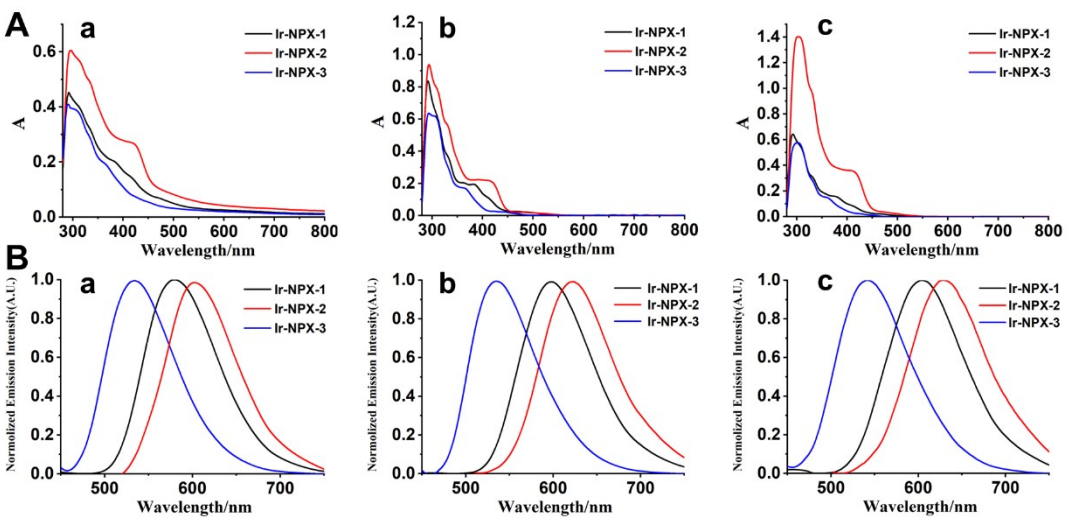

Fig. S12 (A) UV-Vis absorption spectra of **Ir-NPX-1–3** in PBS, CH_2Cl_2, and CH_3CN solutions. (B) Emission spectra of **Ir-NPX-1–3** in PBS, CH_2Cl_2, and CH_3CN solutions (λ_{ex} = 405 nm).

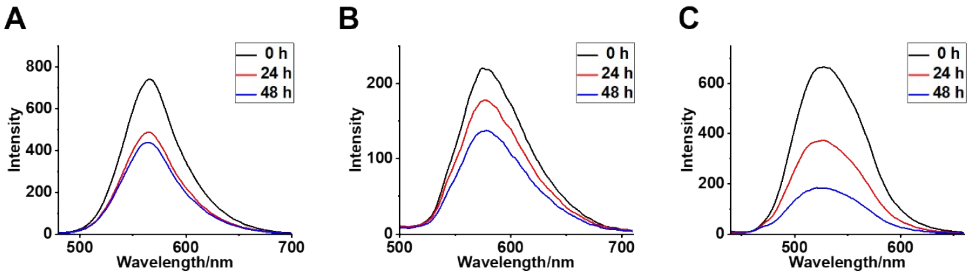

Fig. S13 Emission spectra of **Ir-NPX-1** (A), **Ir-NPX-2** (B) and **Ir-NPX-3** (C) measured in PBS at 0 h, 24 h and 48 h (λ_{ex} = 405 nm).

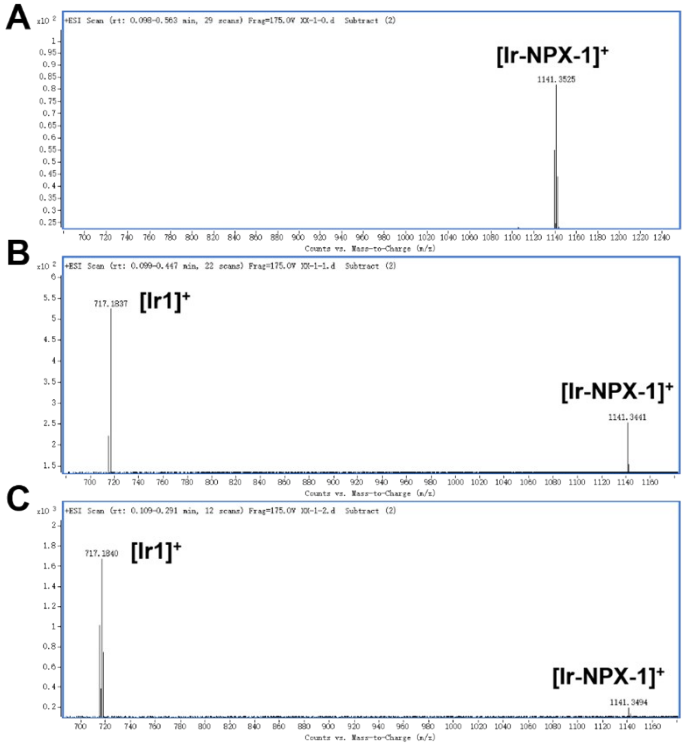

Fig. S14 Mass spectra of **Ir-NPX-1** (20 μM) dispersed in PBS upon treatment with PLE at 298 K for (A) 0 h, (B) 1 h and (C) 2 h.

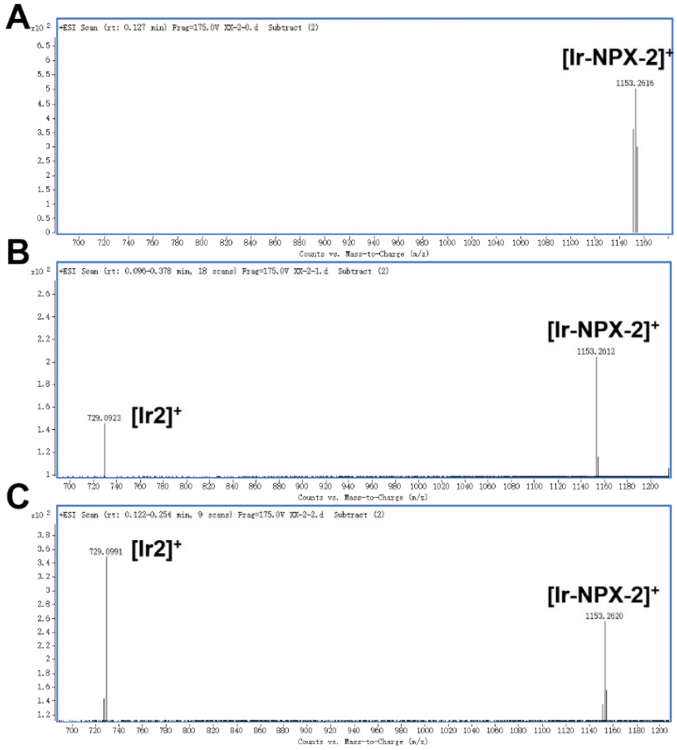

Fig. S15 Mass spectra of **Ir-NPX-2** (20 μM) dispersed in PBS upon treatment with PLE at 298 K for (A) 0 h, (B) 1 h and (C) 2 h.

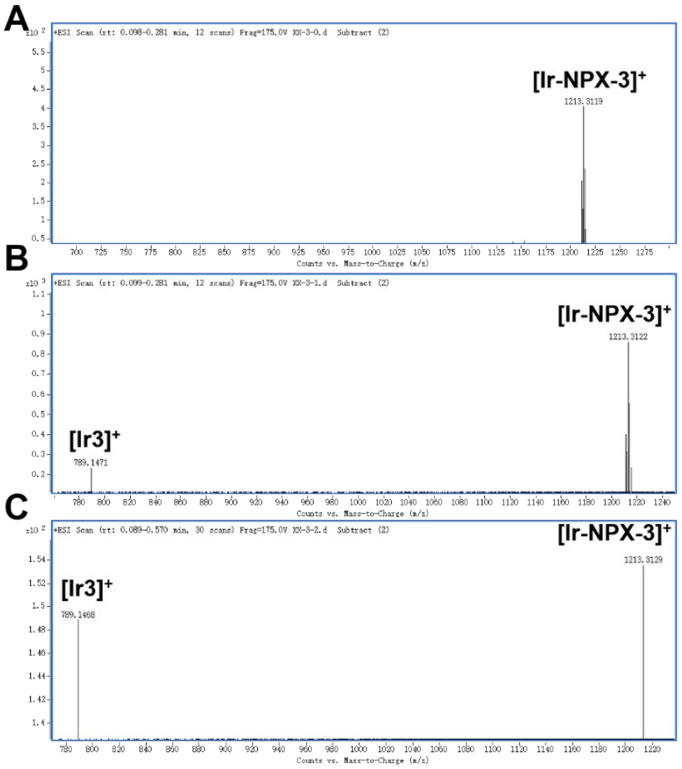

Fig. S16 Mass spectra of **Ir-NPX-3** (20 μM) dispersed in PBS upon treatment with PLE at 298 K for (A) 0 h, (B) 1 h and (C) 2 h.

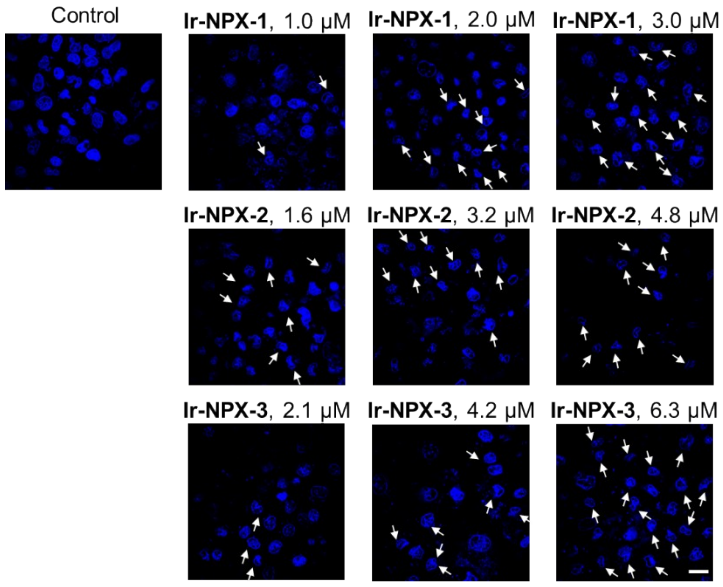

Fig. S17 Observation of the effect of **Ir-NPX-1–3** on cell nucleus by Hoechst 33342 staining (λ_{ex} = 405 nm; λ_{em} = 460 ± 20 nm). Scale bar: 20 μm. The arrows indicate the apoptotic morphological nuclei.

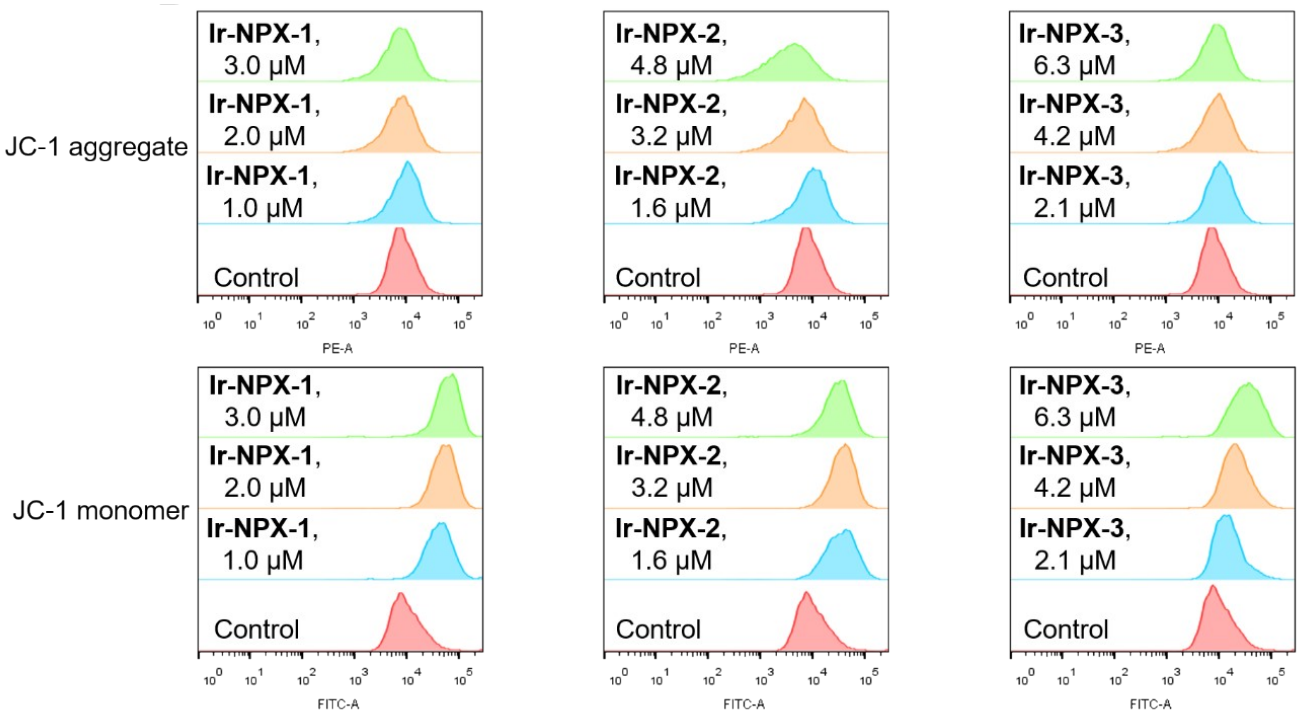

Fig. S18 The effect of **Ir-NPX-1–3** on the change of MMP. A549R cells were treated with **Ir-NPX-1–3** at the indicated concentration for 6 h, then labelled with JC-1, and observed by flow cytometry (λ_{ex} = 488 nm; λ_{em} = 530 ± 20 nm (Green), 585 ± 20 nm (Red)). Scale bar: 20 μm.

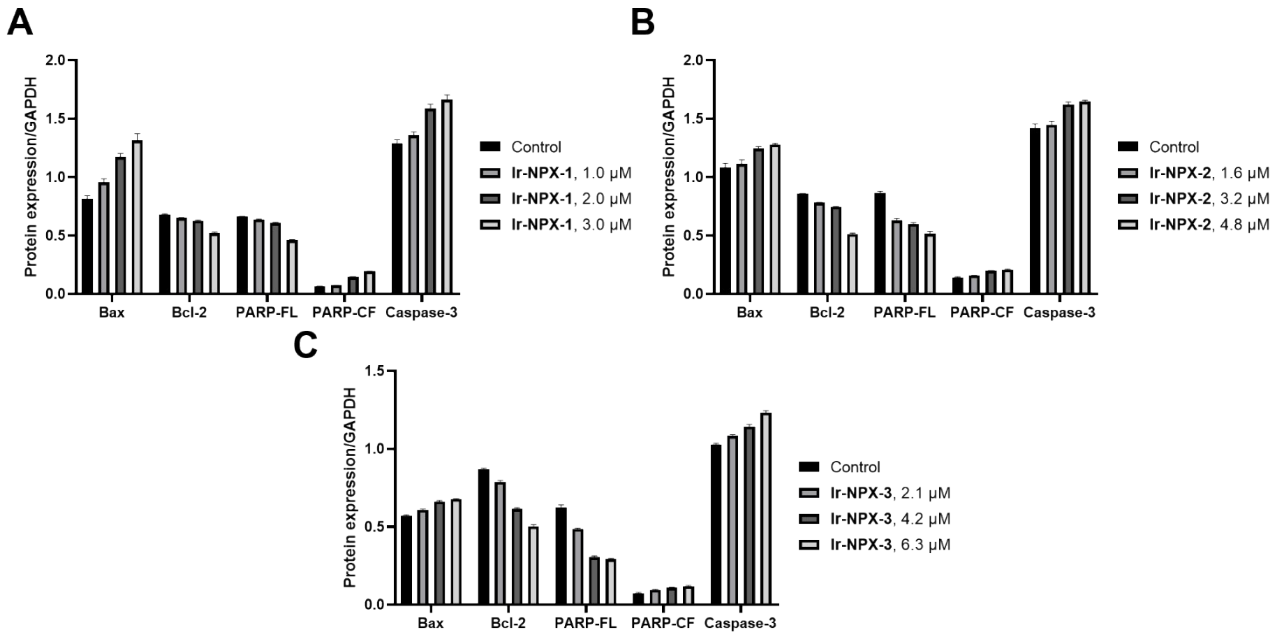

Fig. S19 Histograms of protein expression (Bax, Bcl-2, PARP and Caspase-3) treated with **Ir-NPX-1–3**.

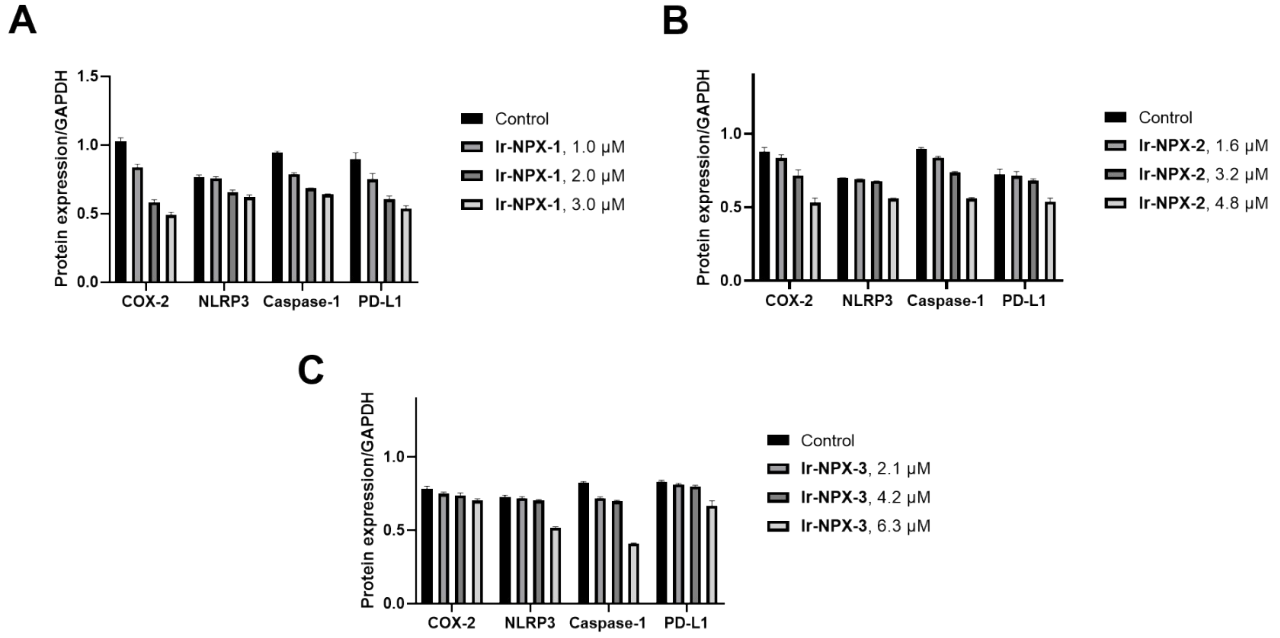

Fig. S20 Histograms of protein expression (COX-2, NLRP3, Caspase-1 and PD-L1) treated with **Ir-NPX-1–3**.

Table S1 Photophysical data of **Ir-NPX-1–3** in PBS, CH_2Cl_2, and CH_3CN

Compounds	Medium	$\lambda_{abs,\ max}$ (nm)	$\lambda_{em,\ max}$ (nm)
Ir-NPX-1	PBS	419	580
	CH_2Cl_2	414	603
	CH_3CN	412	597
Ir-NPX-2	PBS	425	603
	CH_2Cl_2	415	627
	CH_3CN	419	624
Ir-NPX-3	PBS	435	534
	CH_2Cl_2	427	542
	CH_3CN	423	538

Table S2 Antiproliferative activity of tested compounds against cancerous and normal cell lines [a]

Compounds	IC_{50} (μM)				
	HeLa	HepG2	A549	A549R	LO2
Ir1	26.7 ± 0.3	> 100	49.8 ± 0.7	> 100	> 100
Ir2	22.3 ± 0.3	55.8 ± 0.6	24.0 ± 0.4	> 100	> 100
Ir3	6.7 ± 0.1	29.5 ± 1.5	25.8 ± 0.6	31.0 ± 0.5	36.9 ± 0.9
Ir1+NPX	25.6 ± 1.8	> 100	51.6 ± 2.0	> 100	> 100
Ir2+NPX	19.9 ± 1.8	54.9 ± 2.0	23.4 ± 0.9	> 100	> 100
Ir3+NPX	6.3 ± 0.3	28.2 ± 1.4	26.9 ± 0.7	29.7 ± 1.5	34.9 ± 1.6
NPX	> 100	> 100	> 100	> 100	> 100

[a] Data are presented as the mean ± SD of three repeated measurements.

Table S3 Cell-cycle analysis data of **Ir-NPX-1–3** on A549R cells

Compounds	G0/G1	S	G2/M
Control	65.89 ± 3.3	29.98 ± 2.1	4.13 ± 1.2
Ir-NPX-1, 1.0 μM	70.68 ± 3.2	20.57 ± 2.4	8.75 ± 2.3
Ir-NPX-1, 2.0 μM	61.22 ± 3.1	28.78 ± 1.1	10.00 ± 1.2
Ir-NPX-1, 3.0 μM	52.25 ± 2.8	31.05 ± 1.2	16.70 ± 1.3
Ir-NPX-2, 1.6 μM	76.90 ± 6.3	19.30 ± 1.6	3.80 ± 0.7
Ir-NPX-2, 3.2 μM	57.54 ± 3.5	30.37 ± 2.3	12.09 ± 1.4
Ir-NPX-2, 4.8 μM	46.33 ± 3.6	38.71 ± 2.2	14.96 ± 2.3
Ir-NPX-3, 2.1 μM	66.86 ± 3.2	29.11 ± 1.7	4.02 ± 1.9
Ir-NPX-3, 4.2 μM	68.75 ± 2.7	21.10 ± 1.8	10.15 ± 1.6
Ir-NPX-3, 6.3 μM	57.45 ± 6.1	32.24 ± 1.1	10.31 ± 0.3